ACS APPLIED MATERIALS & INTERFACES

Research Article

www.acsami.org

Interface Structure in Cu/Ta_2O_5/Pt Resistance Switch: A First-Principles Study

Bo Xiao* and Satoshi Watanabe

Department of Materials Engineering, The University of Tokyo, Tokyo, Japan

ABSTRACT: The interface structures of a Cu/Ta_2O_5/Pt resistance switch under various oxidation conditions have been examined from first-principles. The O-rich Cu/Ta_2O_5 interface is found to be stable within a wide range of O chemical potentials. In this interface structure, a considerable number of interface Cu atoms tend to migrate to the amorphous Ta_2O_5 (a-Ta_2O_5) layer, which causes the formation of the Cu_2O layer. The interface Cu atoms become more ionized with an increase in the interface O concentration and/or temperature. These ionized Cu^+ ions could function as one of the main sources for the formation of conduction filaments in the Cu/a-Ta_2O_5/Pt resistance switch. In contrast, the ionization of the interface Cu atoms is not observed in the Cu/crystal-Ta_2O_5 interface primarily due to the much lower Cu ionic conductivity in crystal-Ta_2O_5 than that in amorphous state. In addition, the Pt electrode could not be ionized, irrespective of the interface O concentration and temperature. The formation of interface O vacancies in Pt/Ta_2O_5 is always energetically more stable than that in Cu/Ta_2O_5, which may be partly responsible for the cone shape of conduction filament formed in the Cu/a-Ta_2O_5/Pt resistance switch, where the base of the cone lies on the Pt/Ta_2O_5 interface.

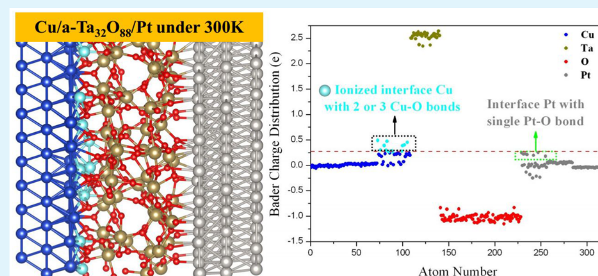

KEYWORDS: *resistance switch, interface structure, amorphous Ta_2O_5, Cu ionization, interface O concentration, metal−oxide heterostructure*

1. INTRODUCTION

In recent years, nanoscale resistance switches, which are constructed with metal−insulator−metal structures, have attracted much attention due to their high scalability, low power consumption, and potential applications in memory cells.[1−3] Resistance switches can be classified into two main types: unipolar and bipolar switches.[4−11] In unipolar switches, which consist of an insulator (TiO_2,[4] NiO,[5] Nb_2O_5,[6] ZrO_2,[7] etc.) sandwiched between two same metal electrodes, the switching direction depends only on the amplitude of the applied voltage. On the other hand, in bipolar switches, the switching can be induced by changing the polarity of the bias voltage applied to either electrode. In general, bipolar switches are designed with an asymmetric structure consisting of an insulator (Cu_2S,[8] Ag_2S,[9] TiO_2,[10] Ta_2O_5,[11] etc.) sandwiched between an oxidizable electrode such as Ag and Cu and an inert electrode such as Pt and Au. In addition, bipolar switches could also be realized without an oxidizable electrode (e.g., Ta/TaO_x/Ir[12] or Hf/HfO_x/TiN).[13]

The switching mechanism of metal−oxide-based resistance switches is still under debate. Several models have been suggested, such as the modification of the Schottky barrier height due to defects or trapped carriers, the alteration of bulk insulator resistivity due to defects or trapped carriers, and the formation of metal/vacancy conduction filament (CF) between two electrodes under electric field.[14]

In the present study, we focus on the resistance switch based on amorphous Ta_2O_5 (a-Ta_2O_5), such as Cu/a-Ta_2O_5/Pt,[11] which is particularly promising as a practical device due to its compatibility with semiconductor fabrication processes. The generally accepted switching mechanism of the Cu/a-Ta_2O_5/Pt resistance switch is based on the formation/annealing of Cu filament under bias voltages[11] in which three rate-limiting processes have been suggested: (1) the ionization/oxidation of Cu at the Cu/a-Ta_2O_5 interface, (2) the migration of Cu ions in the a-Ta_2O_5 layer, and (3) the nucleation of Cu at the Pt/a-Ta_2O_5 interface.[15,16] It should be noted that the initial ionization of Cu atoms in the Cu/a-Ta_2O_5 interface plays an important role in determining the performance of resistance switch because the ionized Cu atoms migrate through the a-Ta_2O_5 layer under the action of electrical bias and are finally reduced at the Pt electrode to form the conductive filament.[15] Moreover, Rodriguez et al.[17] proposed that, for the diffusion of metallic Cu to be enhanced by the action of an electric field into dielectrics, the metal must first be ionized, and the ionization occurs by oxidation.[15,18]

In the present study, to fully understand the ionization/oxidization behavior of the interface Cu atoms, we examine the interface structures and electronic properties of the Cu/a-Ta_2O_5/Pt heterostructures as functions of the interface O concentration and temperature. Our results demonstrate that the O-rich Cu/a-Ta_2O_5 interface structure is stable within a

Received: September 28, 2014
Accepted: December 23, 2014
Published: December 23, 2014

ACS Publications © 2014 American Chemical Society

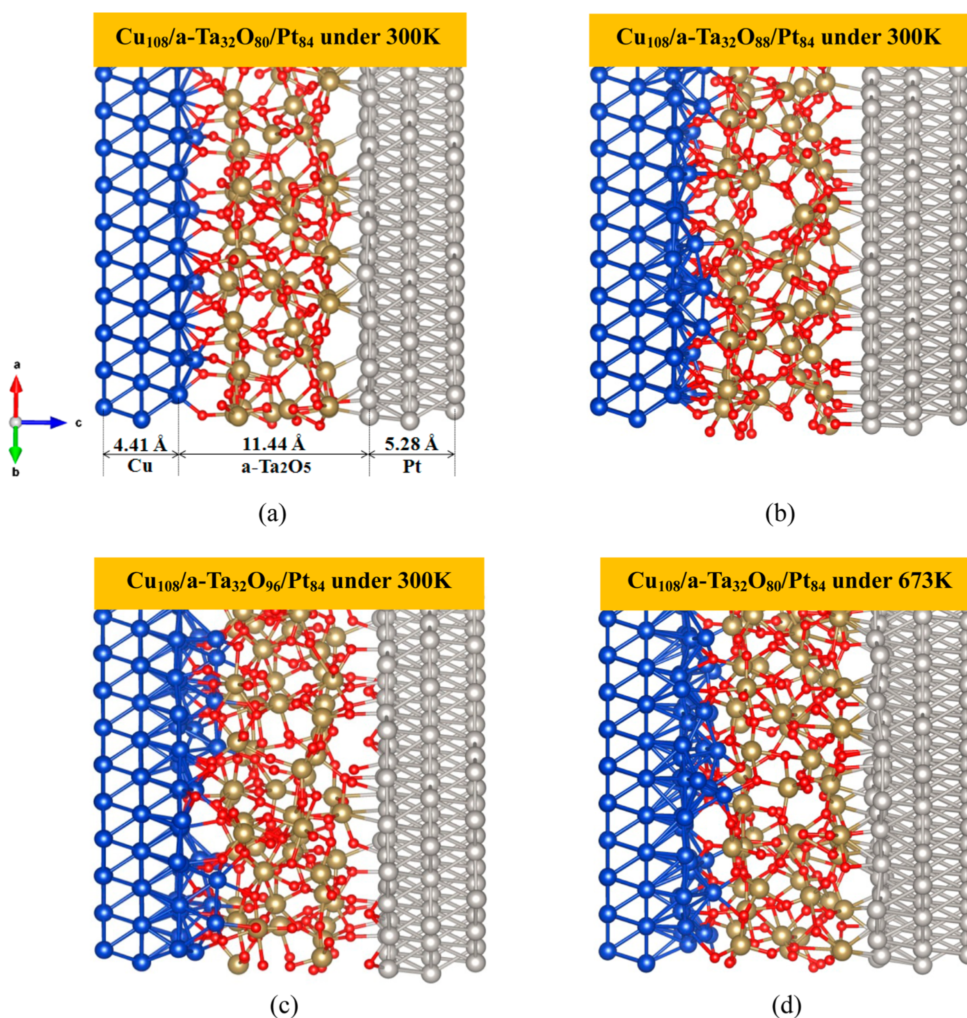

Figure 1. Cu/a-Ta_2O_5/Pt heterostructures of (a) a-O8, (b) a-O12, and (c) a-O16 after molecular dynamic (MD) simulations at 300 K and (d) a-O8 after MD simulations at 673 K. For the definitions of a-O8, a-O12, and a-O16, see the main text.

large range of O chemical potential, and the interface Cu atoms become more ionized with the increase in interface O concentrations and temperatures. As expected, the interface Pt atoms could scarcely be ionized even under O-rich conditions and/or high temperatures. The formation of interface O vacancies is preferred near the Pt/Ta_2O_5 interface as compared with that near the Cu/Ta_2O_5 interface. This may result in the formation of nanoporous structures near the Pt/Ta_2O_5 interface and thus may be partially responsible for the cone shape of the CF formed across the Cu/a-Ta_2O_5/Pt resistive switch, where the base of the cone lies on the Pt/Ta_2O_5 interface.

2. CALCULATION METHODS

All calculations were performed using the Vienna ab initio simulation package (VASP).[19,20] A plane wave basis with cutoff energy of 400 eV was used. The projector augmented-wave (PAW)[21] method and the generalized gradient approximation (PW91)[22] were adopted to describe the electron−ion and electron−electron interactions, respectively.

To investigate the Cu ionization in the Cu/Ta_2O_5 interface, a-Ta_2O_5-based resistance switch models (i.e., Cu/a-Ta_2O_5/Pt) were constructed because the amorphous phase is usually adopted in experiments and prototype devices.[11] First, the Cu/crystal-δ-Ta_2O_5/Pt heterostructure was constructed similarly to that in our previous study.[23] In this model, the system consists of 108 Cu, 96 O, 32 Ta, and 84 Pt atoms. The interface hexagonal unit cell axes are $a = b = 14.67$ Å, and the thickness (along the c axis) of the Cu, Ta_2O_5, and Pt slabs in this heterostructure is 4.41, 11.44, and 7.92 Å, respectively. A 15 Å vacuum region (along the c axis) was used to avoid interactions between the top (Cu) and bottom (Pt) electrodes. Three types of Cu/a-Ta_2O_5/Pt heterostructures with different interface O concentrations were constructed: $Cu_{108}Ta_{32}O_{80}Pt_{84}$ (denoted a-O8), $Cu_{108}Ta_{32}O_{88}Pt_{84}$ (a-O12), and $Cu_{108}Ta_{32}O_{96}Pt_{84}$ (a-O16). Here, a-O8 is constructed from the Cu/c-Ta_2O_5/Pt structure with a stoichiometric c-$Ta_{32}O_{80}$ slab between two electrodes, where both of the Cu/c-Ta_2O_5 and Pt/c-Ta_2O_5 interface O layers contain 8 O atoms. In the a-O12 and a-O16 models, 4 and 8 additional O atoms are introduced into each interface, respectively.

After structure optimization, melt-quenching processes were subsequently performed with fixed Cu (and Pt) layers. The melt-quenching method that was used in the construction of the a-Ta_2O_5 model in our previous study[24] has been successfully applied to these processes. The total simulation time was 22 ps with a time step of 3 fs. Only the Gamma point was used for k-space integrations considering the heavy computational cost and insulator properties of a-Ta_2O_5. Periodic boundary conditions were used with fixed lattice constants. Finally, the obtained Cu/a-Ta_2O_5/Pt heterostructure was further equilibrated at room temperature for 9 ps and then optimized with the relaxation of all of the atoms.

The interface energy of the Cu/Ta_2O_5/Pt heterostructure was calculated from the total energy E_T of the supercell and the atomic chemical potentials of constituent atoms:[24]

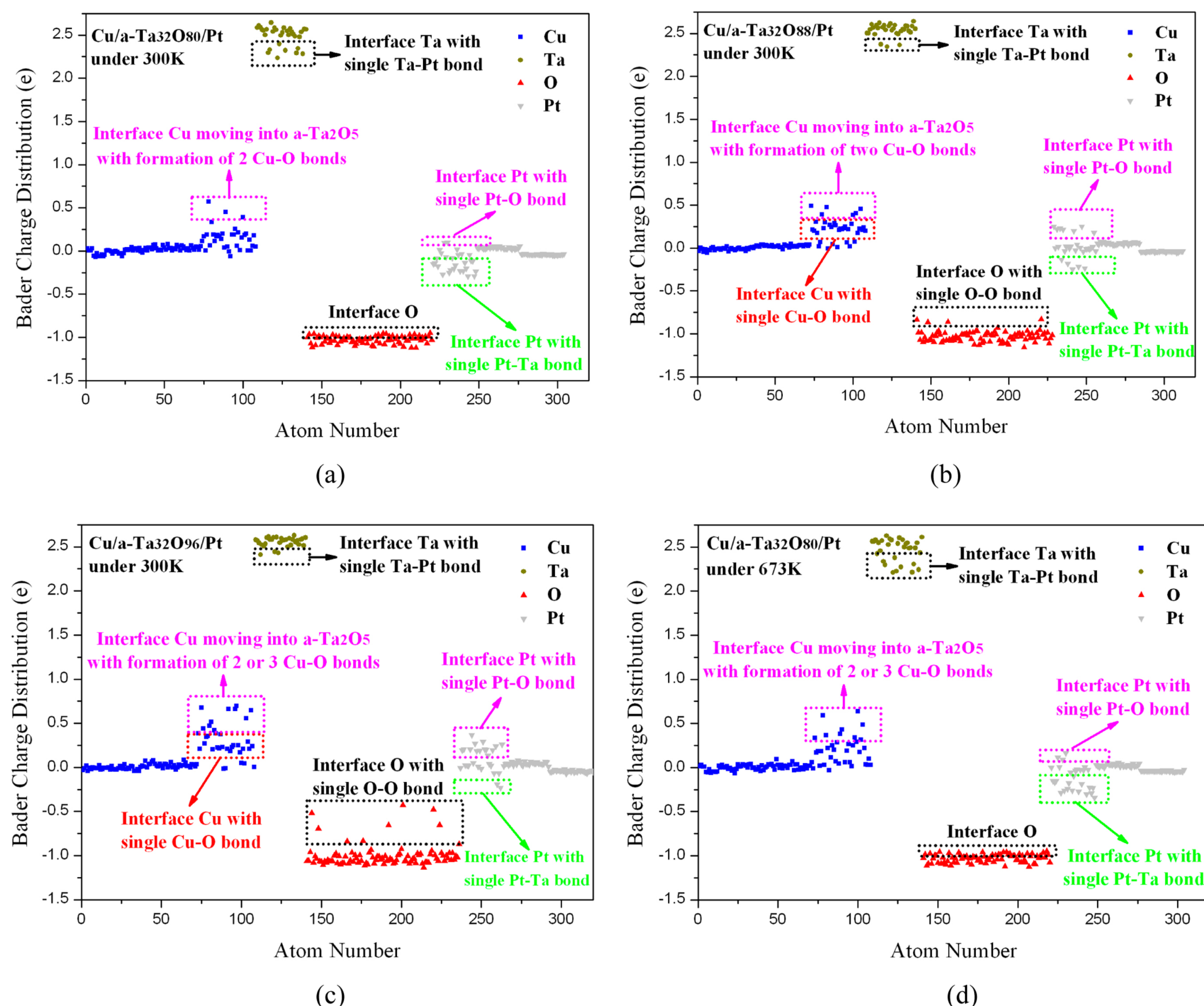

Figure 2. Bader charge distribution of $Cu/a-Ta_2O_5/Pt$ heterostructures of (a) a-O8, (b) a-O12, and (c) a-O16 after molecular dynamic (MD) simulations at 300 K and (d) a-O8 after MD simulations at 673 K.

$$\gamma = E_T - \frac{N_{Ta}}{2}\mu_{Ta_2O_5} - \left(N_O - \frac{5N_{Ta}}{2}\right)\mu_O - N_M\mu_M$$

where N_{Ta}, N_O, and N_M are the numbers of Ta and O atoms in the Ta_2O_5 slab and Cu (or Pt) atoms in the Cu (or Pt) slab, respectively. The following equilibrium condition for bulk Ta_2O_5 is used: $\mu_{Ta_2O_5} = 2\mu_{Ta} + 5\mu_O$, where μ_{Ta} and μ_O are the chemical potentials of Ta and O in the bulk Ta_2O_5. Here, $\mu_{Ta_2O_5}$ and μ_M are the calculated chemical potentials of bulk Ta_2O_5 and metal Cu (or Pt), respectively. The range of μ_O is

$$-\frac{1}{5}\Delta H + \mu_O^{gas} \le \mu_O \le \mu_O^{gas}$$

where ΔH is the heat of formation of Ta_2O_5, which is set to the experimental value of 21.26 eV.[25]

3. RESULTS AND DISCUSSION

The three generated $Cu/a-Ta_2O_5/Pt$ heterostructures are shown in Figure 1. For the stoichiometric case (a-O8, Figure 1a), the O atoms tend to accumulate near the $Cu/a-Ta_2O_5$ interface but are depleted from the $Pt/a-Ta_2O_5$ interface, even though the same interface O concentration was used in the initial $Cu/c-Ta_2O_5/Pt$ heterostructure. As a consequence, only the Cu−O bonding structure appears at the $Cu/a-Ta_2O_5$ interface, while a considerable number of Pt−Ta bonds are formed at the $Pt/a-Ta_2O_5$ interface. At the $Cu/a-Ta_2O_5$ interface, most of Cu atoms bond with single O atom with the averaged Cu−O bond length of 2.15 Å, which is longer than that in the Cu_2O (1.85 Å) system. These Cu atoms are slightly ionized with the average charge transfer from Cu to O atom of ∼0.2 e, as shown in the Bader charge distribution in Figure 2a. We also find that several interface Cu atoms migrate into the a-Ta_2O_5 layer by bonding with two O atoms. The average charge transfer from Cu to O in this case is ∼0.4 e, indicating the strong ionization of these Cu atoms. At the $Pt/a-Ta_2O_5$ interface (Figure 1a), most of Pt atoms obtain electrons from interface Ta atoms due to the formation of Pt−Ta bonds. Meanwhile, the coordination numbers (bonding with O) of these interface Ta atoms decrease by about 1, which results in the reduction of Ta atoms as shown in Figure 2a.

With the increase in the interface O concentration, the structural distortion near the $Cu/a-Ta_2O_5$ interface becomes more significant, as shown in Figure 1, panels b (a-O12) and c

DOI: 10.1021/am5066656
ACS Appl. Mater. Interfaces 2015, 7, 519−525

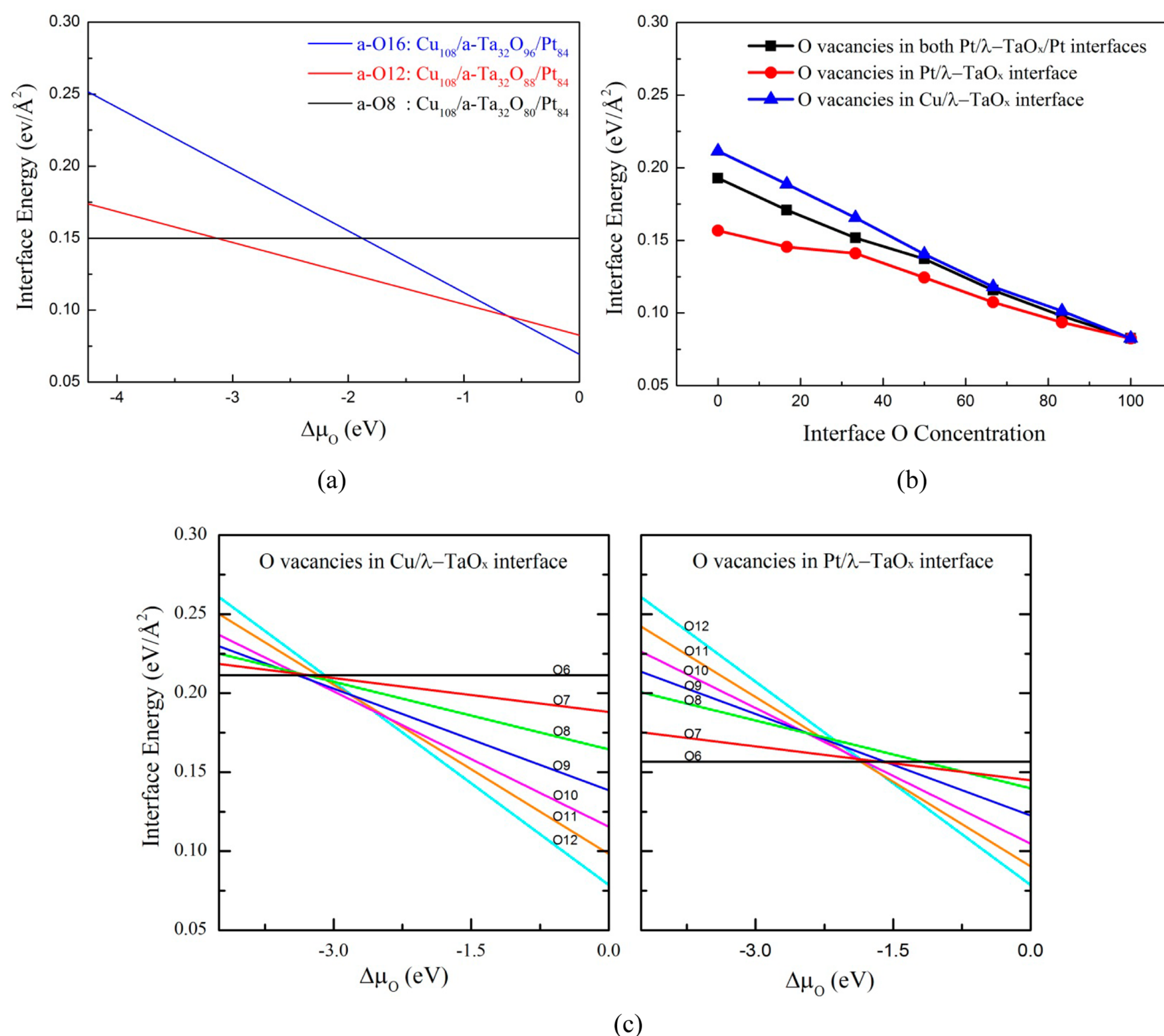

Figure 3. (a) Dependence of the interface energies of a-O8, a-O12, and a-O16 models on the O chemical potential; (b) dependence of the interface energies of Cu/λ-Ta_2O_5/Pt heterostructures on the interface O concentrations; and (c) dependence of the interface energies of Cu/λ-Ta_2O_5/Pt heterostructures with various O concentrations on the O chemical potential.

(a-O16). Due to the relatively high interface O concentration, several Ta–O–O bonding structures are formed at the interfaces of both the a-O12 and a-O16 models, and the corresponding Bader charge analyses (Figure 2b,c) show fewer negative charges on these O ions with O–O bonds than those bonding with metals. We note that a similar Ta–O–O-structure has been experimentally observed in a Cu/a-Ta_2O_5/Pt resistive switch.[26] In both the a-O12 and a-O16 models, the interface Pt atoms are still in their original position irrespective of the interface O concentrations. These Pt atoms with a single Pt–O (Pt–Ta) bond are slightly ionized (reduced) with the averaged charge transfer to the O (Ta) atom is ∼0.2e (−0.25e). In contrast, a considerable number of interface Cu atoms in the a-O12 and a-O16 models have migrated to the a-Ta_2O_5 layer with each Cu atom forming two (this is the predominant case) or three Cu–O bonds. The average Cu–O bond length (1.90 Å) is slightly longer than that in bulk Cu_2O (1.85 Å). The Bader charge analyses reveal that these interface Cu atoms in the a-O12 and a-O16 models have been strongly oxidized, losing ∼0.45 and ∼0.55 e on average, as shown in Figure 2b,c. We note that our calculated Bader charge distribution always underestimates the charges by 50% as compared with the formal valence number: for example, the averaged charges on O and Ta atoms are about −1e and 2.5e, respectively, which are only half of the formal valence of O^{2-} and Ta^{5+} ions in a-Ta_2O_5. Accordingly, the interface Cu atoms with 0.45e and 0.55e charges can be regarded as $Cu^{0.9+}$ and $Cu^{1.1+}$ ions, respectively. Moreover, the experimental study has also confirmed that the thermally diffused Cu in a-Ta_2O_5 exists as Cu^+ ions.[26] Thus, our results reveal that the Cu suboxide layer (i.e., Cu_2O) can be formed in the Cu/a-Ta_2O_5 interface under O-rich interface conditions. In a real Cu/a-Ta_2O_5/Pt device, a certain amount of residual water is present in the a-Ta_2O_5 layers, which is absorbed from the ambient air.[15] According to the experiments, moisture within an oxide film has an important impact on the Cu injection and redox reaction in resistance switches.[15,27,28] In the present study, we show an increase of the interface O concentration at the Cu/a-Ta_2O_5 interface. We note that the

DOI: 10.1021/am5066656
ACS Appl. Mater. Interfaces 2015, 7, 519–525

introduction of water into the Cu/a-Ta_2O_5 interface could further increase the interface O concentration, and thus, it is reasonable to conclude that the Cu electrode would likely undergo chemical oxidization via the interface water.[15] In addition, the water reduction reaction at the Pt electrode could also provide the counter charge supply required for Cu ion formation at the electrode interface.[27,28] Similar results are expected to be obtained in Cu/SiO_2/Pt resistance switches[29] because both Ta_2O_5- and SiO_2-based devices have shown similar behavior concerning the switching properties and the effects of moisture.

We also know that temperature is another key element affecting the switching performance of the Cu/a-Ta_2O_5/Pt resistance switch. For example, the magnitude of the SET voltage of the Cu/a-Ta_2O_5/Pt resistance switch decreases with increasing temperature,[15] which can be partly attributed to the increase in the diffusion speed of Cu in a-Ta_2O_5 at high temperatures. Therefore, the temperature effect on the ionization and migration of interface Cu atoms is examined. The structure of the a-O8 model after 2 ps of molecular dynamics (MD) simulation at 673 K is shown in Figure 1d. More interface Cu atoms have migrated into the a-Ta_2O_5 layer with a longer distance as compared with the original a-O8 model (Figure 1a). This migration is associated with a stronger ionization of the interface Cu atoms, as shown in Figure 2d. Thus, the temperature is another method for controlling the ionization of the interface Cu atoms.

Next, we would like to discuss the stability of the Cu/a-Ta_2O_5/Pt heterostructures as a function of the interface O concentration. The calculated interface energies are shown in Figure 3a, revealing that the a-O12 model is the most stable model within a large O chemical potential range and that the a-O8 and a-O16 models can only appear under extremely O-deficient and O-rich conditions, respectively. As mentioned above, O atoms tend to accumulate at the Cu/a-Ta_2O_5 interface, and as a consequence, the interface O concentration in the a-O12 model is very high. Thus, it is reasonable to conclude that the O-rich interface structure of Cu/a-Ta_2O_5, in which the Cu_2O layer is formed, is energetically preferable. In addition, our results on the accumulation (depletion) of oxygen at the Cu/Ta_2O_5 (Pt/Ta_2O_5) interface can be understood in terms of the band bending. Because Pt has a high work function, the energy bands of Ta_2O_5 near the Pt/Ta_2O_5 interface should bend upward, and positive charges should accumulate near this interface. On the other hand, the downward bending of the band, and thus the accumulation of negative charges, should occur near the Cu/Ta_2O_5 interface. Our first-principles simulations show that such charge accumulation is achieved via accumulation of oxygen or oxygen vacancies in the present situation. Similar behavior has been observed in theoretical studies on the metal/yttrium-stabilized zirconia interface.[30,31]

For further understanding of the stability, it may be useful to examine the Cu/Ta_2O_5/Pt heterostructures with a well-defined interface. For this purpose, computational models are constructed based on crystalline λ-Ta_2O_5, which is the most stable structure among all predicted low-temperature crystalline Ta_2O_5 structures.[32,33] The chemical component of this heterostructure is $Cu_{69}/Ta_{36}O_{102}/Pt_{63}$. Because the λ-Ta_2O_5 slab, which we cleaved, contains 12 O atoms per supercell; it is denoted as c-O12. Subsequently, several Cu/λ-Ta_2O_5/Pt heterostructures are constructed by removing interface O atoms from either one interface or from both interfaces. As shown in Figure 3b, the formation of O vacancies in the Pt/λ-Ta_2O_5 interface is always energetically more stable than that in Cu/λ-Ta_2O_5, and the O-rich interface in Cu/λ-Ta_2O_5 is stable within larger O chemical potential range than that of Pt/λ-Ta_2O_5, as shown in Figure 3c. These results further confirm the different O preference between the Pt/Ta_2O_5 and Cu/Ta_2O_5 interfaces, which corresponds to the results of the amorphous cases discussed above.

We further note that the ionization behavior of both the interface Cu and Pt atoms could not be found in Cu/λ-Ta_2O_5/Pt, irrespective of the interface O concentration or temperature, which is likely due to the different Cu ionic conductivity in crystalline and amorphous Ta_2O_5. In room-temperature experiments, the Cu ionic conductivity was found to be negligible in crystalline Ta_2O_5[34,35] but enhanced in the amorphous case due to its lower density than the bulk state.[36] Considering the absence of ionized Cu atoms near Cu/c-Ta_2O_5 interface, our results further provide the disadvantages of crystalline-Ta_2O_5 for a Cu ion-conducting solid electrolyte.[37]

As mentioned above, O atoms tend to accumulate near the Cu/a-Ta_2O_5 interface but are depleted from the Pt/a-Ta_2O_5 interface because the formation of O vacancies near the Pt/Ta_2O_5 interface is energetically more favorable than that near the Cu/Ta_2O_5 interface. Specifically, in the case of the most stable a-O12 structure (Figure 4a,b), the calculated O coverage on the interface Cu and Pt layers is 86 and 29%, respectively (here, the O coverage value is defined as the number of metal

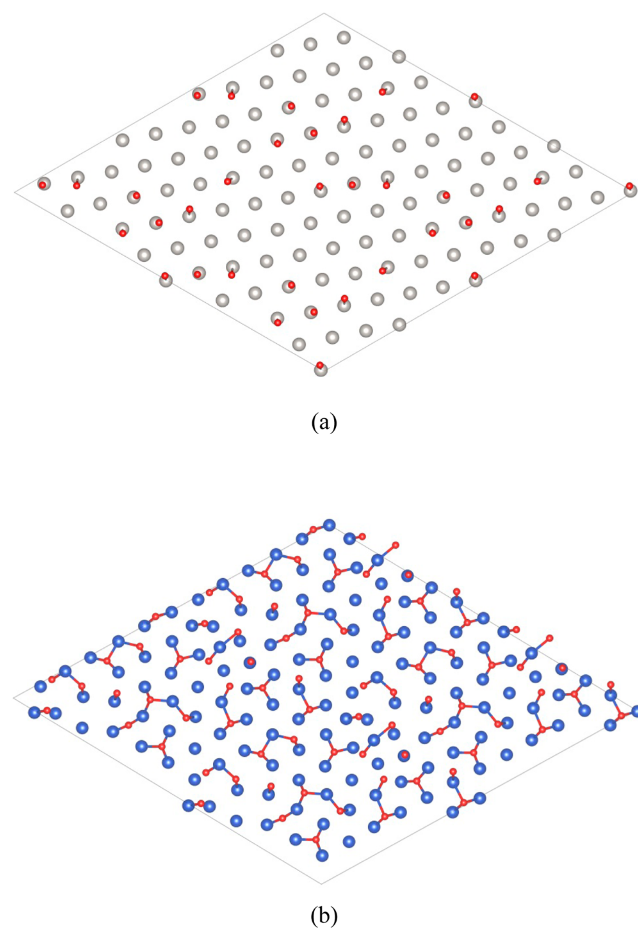

Figure 4. Top views of the interface O distribution on (a) Pt and (b) Cu slabs in the a-O12 model.

DOI: 10.1021/am5066656
ACS Appl. Mater. Interfaces 2015, 7, 519−525

atoms with metal−O bonds divided by the total number of interface metal atoms). In particular, a wide area of interface Pt atoms with no Pt−O bonding is observed in the Pt/a-Ta_2O_5 interface shown in Figure 4a, which may result in the formation of the sparse structure shown in Figure 1b. Similar O vacancy coalescence has been widely used to explain the formation of nanopores in materials such as $BaTiO_3$,[38] ZnO,[39] Si/SiO_2,[40] Al_2O_3/FeAl,[41] and CeO_2/ITO.[42] In contrast, a dense structure with smaller void spaces (or nanopores with small diameters) is formed near the Cu/a-Ta_2O_5 interface, as shown in Figure 1b, which can be attributed to the lack of vacancies shown in Figure 4b. Thus, we propose that the formation of different sized nanopores may occur in the interfaces of Cu/a-Ta_2O_5/Pt during fabrication. Because the switching mechanism of the Cu/a-Ta_2O_5/Pt device is based on the diffusion of Cu ions across the nanopores in a-Ta_2O_5, the Cu ions first nucleate near the Pt/a-Ta_2O_5 interface.[15] Thus, considering the obviously different porosities (or O coverage) between the Pt/Ta_2O_5 and Cu/Ta_2O_5 interfaces, the diameter of the Cu conduction filament (CF) in a-Ta_2O_5 is not likely to be uniform, that is, the CF is thicker near the Pt/a-Ta_2O_5 interface and thinner near the Cu/a-Ta_2O_5 interface, which corresponds to the experimental results where a cone-shaped CF was observed.[11]

We next consider the electronic properties of Cu/a-Ta_2O_5/Pt heterostructure. For simplicity, we only consider the a-O12 model. As shown in Figure 5a, the density of states (DOS) around the Fermi level primarily consists of the Cu, Pt, and interface O atoms. This suggests strong hybridization between Cu (Pt) and the interface O states, which is consistent with the obvious charge transfer at the interface region. As a result, the interface system shows metallic behavior, and the gap states primarily arise from the interfacial Cu−O, Pt−O, and Pt−Ta bonding, as shown in Figure 5b,c. This metallic behavior occurs because only few Pt−Ta bonds are formed at the O-rich interface of Pt/a-Ta_2O_5. In the central region, neither the O atoms nor the Ta atoms contribute near the Fermi level (Figure 5d), indicating the insulator properties of a-Ta_2O_5.

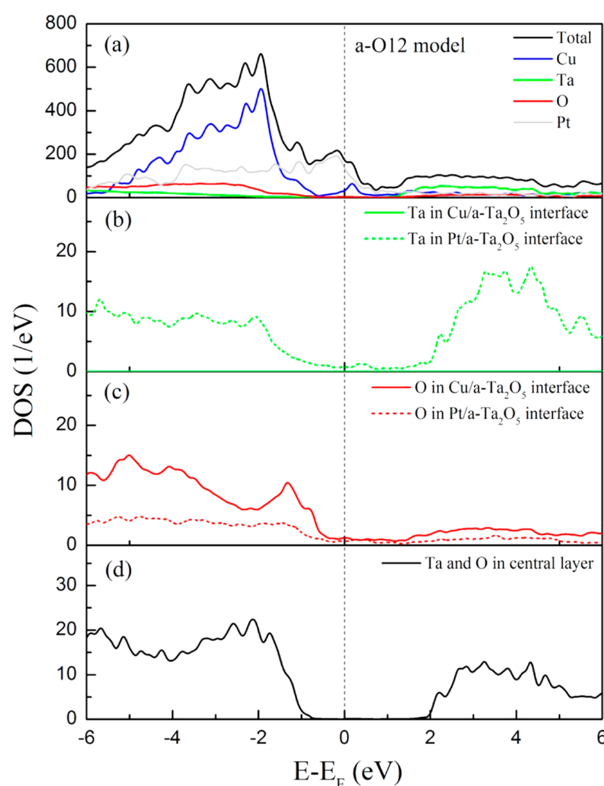

Figure 5. (a) The total density of states (DOS) and partial DOS of each element (including Cu, Ta, O, and Pt) in the a-O12 model, and the partial DOS of (b) Ta in both interfaces, (c) O in both interfaces, and (d) Ta and O in the central layer of the a-O12 model.

4. CONCLUSION

We have investigated the structure and electronic properties of the interfaces in a Cu/a-Ta_2O_5/Pt resistance switch. Our results reveal that the O-rich interface is preferable in Cu/a-Ta_2O_5 in a wide range of O chemical potential, in which a considerable number of interface Cu atoms tend to migrate into a-Ta_2O_5 with the formation of the Cu_2O layer. In addition, the ionization of the interface Cu atoms is enhanced with increasing interface O concentration and temperature. In contrast, the interface Cu atoms could not be ionized in the Cu/c-Ta_2O_5, which results in the switching failure of the Cu/c-Ta_2O_5/Pt resistance switch. In both the Pt/a-Ta_2O_5 and Pt/c-Ta_2O_5 interfaces, the Pt atoms could hardly be oxidized, irrespective of interface O concentration or temperature. The formation of interface O vacancies in Pt/Ta_2O_5 is always energetically more stable than that in Cu/Ta_2O_5, which results in a significantly different O coverage in the Pt/Ta_2O_5 (29%) and Cu/Ta_2O_5 (86%) interfaces. This difference in O coverage may be partly responsible for the cone-shaped Cu conduction filament with the base of the cone on the Pt/Ta_2O_5 interface.

■ AUTHOR INFORMATION

Corresponding Author

*E-mail: xiaobo@cello.t.u-tokyo.ac.jp.

Notes

The authors declare no competing financial interest.

■ ACKNOWLEDGMENTS

This work was partially supported by CREST-JST “Atom transistor,” Low Power Electronics Association and Projects, the Grant-in-Aid for Innovation Area “Computics” by MEXT, Japan. Part of the computations in this work was performed using the facilities of the Supercomputer Center, the Institute for Solid State Physics, the University of Tokyo.

■ REFERENCES

(1) Terabe, K.; Hasegawa, T.; Nakayama, T.; Aono, M. Quantized Conductance Atomic Switch. *Nature* **2005**, *433*, 47−50.
(2) Waser, R.; Aono, M. Nanoionics-Based Resistive Switching Memories. *Nat. Mater.* **2007**, *6*, 833−840.
(3) Sawa, A. Resistive Switching in Transition Metal Oxides. *Mater. Today.* **2008**, *11*, 28−36.
(4) Rohde, C.; Choi, B. J.; Jeong, D. S.; Choi, S.; Zhao, J.-S.; Hwang, C. S. Identification of a Determining Parameter for Resistive Switching of TiO_2 Thin Films. *Appl. Phys. Lett.* **2005**, *86*, 262907.
(5) Seo, S.; Lee, M. J.; Seo, D. H.; Jeoung, E. J.; Suh, D. S.; Joung, Y. S.; Yoo, I. K.; Hwang, I. R.; Kim, S. H.; Byun, I. S.; Kim, J.-S.; Choi, J. S.; Park, B. H. Reproducible Resistance Switching in Polycrystalline NiO Films. *Appl. Phys. Lett.* **2004**, *85*, 5655.
(6) Sim, H.; Lee, D.; Seo, S.; Lee, M.-J.; Yoo, I.-K.; Hwang, H. Resistance Switching Characteristics of Polycrystalline Nb_2O_5 for Nonvolatile Memory Applications. *IEEE Electron Device Lett.* **2005**, *26*, 292−294.
(7) Lee, D.; Choi, H.; Sim, H.; Choi, D.; Hwang, H.; Lee, M.-J.; Seo, S.-A.; Yoo, I. K. Resistance Switching of the Nonstoichiometric

DOI: 10.1021/am5066656
ACS Appl. Mater. Interfaces 2015, 7, 519−525

Zirconium Oxide for Nonvolatile Memory Applications. *IEEE Electron Device Lett.* **2005**, *26*, 719–721.
(8) Sakamoto, T.; Sunamura, H.; Kawaura, H.; Hasegawa, T.; Nakayama, T.; Aono, M. Nanometer-Scale Switches Using Copper Sulfide. *Appl. Phys. Lett.* **2003**, *82*, 3032–3034.
(9) Xu, Z.; Bando, Y.; Wang, W. L.; Bai, X. D.; Golberg, D. Real-Time In Situ HRTEM-Resolved Resistance Switching of Ag_2S Nanoscale Ionic Conductor. *ACS Nano* **2010**, *4*, 2515–2522.
(10) Hsiung, C. P.; Liao, H. W.; Gan, J. Y.; Wu, T. B.; Hwang, J. C.; Chen, F.; Tsai, M. J. Formation and Instability of Silver Nanofilament in Ag-Based Programmable Metallization Cells. *ACS Nano* **2010**, *4*, 5414–5420.
(11) Sakamoto, T.; Lister, K.; Banno, N.; Hasegawa, T.; Terabe, K.; Aono, M. Electronic Transport in Ta_2O_5 Resistive Switch. *Appl. Phys. Lett.* **2007**, *91*, 092110.
(12) Ninomiya, T.; Muraoka, S.; Wei, Z.; Yasuhara, R.; Katayama, K.; Takagi, T. Improvement of Data Retention During Long-Term Use by Suppressing Conductive Filament Expansion in TaO_x Bipolar-ReRAM. *IEEE Electron Device Lett.* **2013**, *34*, 762–764.
(13) Chen, Y.; Goux, L.; Clima, S.; Govoreanu, B.; Degraeve, R.; Kar, G.; Fantini, A.; Groeseneken, G.; Wouters, D.; Jurczak, M. Endurance/Retention Trade-off on HfO_2-Metal Cap 1T1R Bipolar RRAM. *IEEE Trans. Electron Devices* **2013**, *60*, 1114–1121.
(14) Prakash, A.; Jana, D.; Maikap, S. TaO_x-based Resistive Switching Memories: Prospective and Challenges. *Nanoscale Res. Lett.* **2013**, *8*, 418–434.
(15) Tsuruoka, K.; Terabe, K.; Hasegawa, T.; Valov, L.; Waser, R.; Aono, M. Effects of Moisture on the Switching Characteristics of Oxide-Based, Gapless-Type Atomic Switches. *Adv. Funct. Mater.* **2012**, *22*, 70–77.
(16) Menzel, S.; Tappertzhofen, S.; Waser, R.; Valov, I. Switching Kinetics of Electrochemical Metallization Memory Cells. *Phys. Chem. Chem. Phys.* **2013**, *15*, 6945–6952.
(17) Rodriguez, O. R.; Cho, W.; Saxena, R.; Plawsky, J. L.; Gill, W. N. Mechanism of Cu Diffusion in Porous Low-k Dielectrics. *J. Appl. Phys.* **2005**, *98*, 024108.
(18) Willis, B. G.; Lang, D. V. Oxidation Mechanism of Ionic Transport of Copper in SiO_2 Dielectrics. *Thin Solid Films* **2004**, *467*, 284–293.
(19) Kresse, G.; Furthmüller, J. Efficiency of ab Initio Total Energy Calculations for Metals and Semiconductors Using a Plane-Wave Basis Set. *Comput. Mater. Sci.* **1996**, *6*, 15–50.
(20) Kresse, G.; Furthmüller, J. Efficient Iterative Schemes for ab Initio Total-Energy Calculations Using a Plane-Wave Basis Set. *Phys. Rev. B* **1996**, *54*, 11169–11186.
(21) Kresse, G.; Joubert, J. From Ultrasoft Pseudopotentials to the Projector Augmented-Wave Method. *Phys. Rev. B* **1999**, *59*, 1758–1775.
(22) Wang, Y.; Perdew, J. P. Correlation Hole of the Spin-Polarized Electron Gas, with Exact Small-Wave-Vector and High-Density Scaling. *Phys. Rev. B* **1991**, *44*, 13298–13307.
(23) Gu, T. K.; Wang, Z. C.; Tada, T.; Watanabe, S. First-Principles Simulations on Bulk Ta_2O_5 and $Cu/Ta_2O_5/Pt$ Heterojunction: Electronic Structures and Transport Properties. *J. Appl. Phys.* **2009**, *106*, 103713.
(24) Xiao, B.; Gu, T. K.; Tada, T.; Watanabe, S. Conduction Paths in Cu/Amorphous-Ta_2O_5/Pt Atomic Switch: First-Principles Studies. *J. Appl. Phys.* **2014**, *115*, 034503.
(25) Hong, H. S.; Lee, K. S. Thermodynamic Evaluation of the Ta-O System from Pure Tantalum to Tantalum Pentoxide. *J. Alloys Compd.* **2003**, *360*, 198–204.
(26) Banno, N.; Sakamoto, T.; Iguchi, N.; Matsumoto, M.; Imai, H.; Ichihashi, T.; Fujieda, S.; Tanaka, K.; Watanabe, S.; Yamaguchi, S.; Hasegawa, T.; Aono, M. Structure Characterization of Amorphous Ta_2O_5 and SiO_2-Ta_2O_5 Used as Solid Electrolyte for Nonvolatile Switches. *Appl. Phys. Lett.* **2010**, *97*, 113507.
(27) Tappertzhofen, S.; Waser, R.; Valov, I. Impact of Counter Electrode Material on the Redox Processes in Resistive Switching Memories. *ChemElectroChem.* **2014**, *1*, 1287–1292.
(28) Tappertzhofen, S.; Valov, I.; Tsuruoka, T.; Hasegawa, T.; Waser, R.; Aono, M. Generic Relevance of Counter Charges for Cation-Based Nanoscale Resistive Switching Memories. *ACS Nano* **2013**, *7*, 6396–6402.
(29) Cho, D. Y.; Tappertzhofen, S.; Waser, R.; Valov, I. Bond Nature of Active Metal Ions in SiO_2-based Electrochemical Metallization Memory Cells. *Nanoscale* **2013**, *5*, 1781–1784.
(30) Kasamatsu, S.; Tada, T.; Watanabe, S. Theoretical Analysis of Space Charge Layer Formation at Metal/Ionic Conductor Interfaces. *Solid State Ionics* **2011**, *183*, 20–25.
(31) Kasamatsu, S.; Tada, T.; Watanabe, S. Parallel-Sheets Model Analysis of Space Charge Layer Formation at Metal/Ionic Conductor Interfaces. *Solid State Ionics* **2012**, *226*, 62–70.
(32) Lee, S.; Kim, J.; Kim, S.; Kim, S.; Park, G. Hidden Structure Order in Orthorhombic Ta_2O_5. *Phys. Rev. Lett.* **2013**, *110*, 235502.
(33) Kim, J.; Magyari-Koepe, B.; Lee, K.; Kim, H.; Lee, S.; Nishi, Y. Electronic Structure and Stability of Low Symmetry Ta_2O_5 Polymorphs. *Phys. Status Solidi RRL.* **2014**, *8*, 560–565.
(34) Banerjee, S.; Shen, B.; Chen, I.; Bohlman, J.; Brown, G.; Doering, R. Conduction Mechanisms in Sputtered Ta_2O_5 on Si with an Interfacial SiO_2 Layer. *J. Appl. Phys.* **1989**, *65*, 1140.
(35) Chiu, F.; Wang, J.; Lee, J. Y.; Wu, S. C. Leakage Currents in Amorphous Ta_2O_5 Thin Flms. *J. Appl. Phys.* **1997**, *81*, 6911.
(36) Ngaruiya, J. M.; Venkataraj, S.; Drese, R.; Kappertz, O.; Leervad, P. T. P.; Wuttig, M. Preparation and Characterization of Tantalum Oxide Films Produced by Reactive DC Magnetron Sputtering. *Phys. Status Solidi A* **2003**, *198*, 99–110.
(37) Tsuruoka, T.; Terabe, K.; Hasegawa, T.; Aono, M. Forming and Switching Mechanisms of a Cation-Migration-based Oxide Resistive Memory. *Nanotechnology* **2010**, *21*, 425205.
(38) Hennings, D. F. K.; Metzmacher, C.; Schreinemacher, B. S. Defect Chemistry and Microstructure of Hydrothermal Barium Titanate. *J. Am. Ceram. Soc.* **2001**, *84*, 179–182.
(39) Richardson, J. J.; Goh, G. K. L.; Le, H. Q.; Liew, L. L.; Lange, F. F.; Denbaars, S. P. Thermally Induced Pore Formation in Epitaxial ZnO Films Grown from Low Temperature Aqueous Solution. *Cryst. Growth Des.* **2011**, *11*, 3558–3563.
(40) Mehonic, A.; Cueff, S.; Wojdak, M.; Hudziak, S.; Jambois, O.; Labbe, C.; Garrido, B.; Rizk, R.; Kenyon, A. J. Resistive Switching in Silicon Suboxide Films. *J. Appl. Phys.* **2012**, *111*, 074507.
(41) Hou, P. Y.; Niu, Y.; Lienden, C. V. Analysis of Pore Formation at Oxide-Alloy Interface-I: Experimental Results on FeAl. *Oxid. Met.* **2002**, *59*, 41–61.
(42) Ansari, A. A.; Kaushik, A.; Solanki, P. R.; Malhotra, B. D. Sol–Gel Derived Nanoporous Cerium Oxide Film for Application to Cholesterol Biosensor. *Electrochem. Commun.* **2008**, *10*, 1246–1249.

DOI: 10.1021/am5066656
ACS Appl. Mater. Interfaces 2015, 7, 519–525